J Chem Crystallogr (2014) 44:360–367
DOI 10.1007/s10870-014-0523-5

ORIGINAL PAPER

9,10-Dihydro-8H-11-oxa-cyclohepta[*a*]naphthalen-7-one: Crystallographic, Computational and Hirshfeld Surface Analysis

A. S. Aditya · Manoj Trivedi · Abhinav Kumar

Received: 20 November 2013 / Accepted: 12 June 2014 / Published online: 24 June 2014

Abstract 9,10-Dihydro-8H-11-oxa-cyclohepta[*a*]naphthalen-7-one has been synthesized and characterized by elemental analysis, IR, ^{1}H NMR spectroscopy, mass spectrometry and finally by X-ray crystallography. X-ray diffraction studies indicates that the molecule is stabilized by C–H···O and C–H···π non-covalent interactions in the solid state. Quantum chemical calculations and Hirshfeld surface analysis have been performed to gain insight into the behavior of these weak interactions.

Keywords α-Naphthol · Eaton's reagent · Non-covalent interactions · DFT · AIM · Hirshfeld surface

Introduction

Non covalent interactions are subject of wide interest especially in molecules having aromatic moieties. The generation of such molecular scaffolds using non-bonded interactions is a prevalent theme in the chemical science today. Progress realized in this area has emerged from the concerted efforts of many literature reports to produce the existing database of known patterns of association [1–10].

9,10-Dihydro-8H-11-oxa-cyclohepta[*a*]naphthalen-7-one has been synthesized and utilized as the starting material for generation of variety of molecular scaffolds displaying variety of interactions in the solid state [11–15]. Still there are no reports to address the nature of weak interactions existing in this molecule. Staying with these facts in mind herein we wish to report the relatively improved synthesis, characterization and X-ray structure of the title compound. Particular attention has been devoted to address the behaviour of weak interactions with the aid of density functional theory (DFT), atoms-in-molecules (AIM) and Hirshfeld surface analysis.

Experimental

Materials and Physical Measurements

All the synthetic manipulations were performed under ambient atmosphere. The solvents were dried and distilled before use by following the standard procedures. IR as KBr pellet and ^{1}H NMR spectra were recorded on a Varian 3100 FTIR spectrophotometer and JEOL AL300 FTNMR spectrometer, respectively. Chemical shifts were reported in parts per million using TMS as internal standard. Elemental analysis was performed on Exeter analytical Inc. "Model CE-440 CHN analyser".

X-Ray Crystallographic Study

Intensity data for the colourless crystals of title compound was collected at 100(2) K on a Bruker SMART diffractometer system equipped with graphite monochromated Mo Kα radiation λ = 0.71073 Å. The final unit cell determination, scaling of the data, and corrections for

A. S. Aditya
Institut für Chemie, TU Berlin, 10623 Berlin, Germany

M. Trivedi
Department of Chemistry, University of Delhi, Delhi 110 001, India

A. Kumar (✉)
Department of Chemistry, Faculty of Science, University of Lucknow, Lucknow 226 007, India
e-mail: abhinavmarshal@gmail.com;
kumar_abhinav@lkouniv.ac.in

Lorentz and polarization effects were performed with Bruker SAINT [16]. A symmetry-related (multi-scan) absorption correction had been applied. Structure solution, followed by full-matrix least squares refinement was performed using the WINGX-1.70 suite [17] of programs throughout. All non-hydrogen atoms were refined anisotropically; hydrogen atoms were located at calculated positions and refined using a riding model with isotropic thermal parameters fixed at 1.2 times the Ueq value of the appropriate carrier atom. Figure was prepared using ORTEP [18]. Crystal data for the title compound: $C_{14}H_{12}O_2$, formula mass 212.24, orthorhombic space group Pbca, $a = 12.012(3)$, $b = 8.5385(19)$, $c = 20.189(5)$ Å, $V = 2{,}070.6(8)$ Å^3, $Z = 8$, $d_{\text{calcd}} = 1.362$ mg m^{-3}, linear absorption coefficient 0.090 mm^{-1}, $F(000) = 896$, crystal size 0.35 × 0.20 × 0.15 mm, reflections collected 12596, independent reflections 2540 [$R_{\text{int}} = 0.0737$], Final indices [$I > 2\sigma(I)$] $R_1 = 0.0553$ $wR_2 = 0.1337$, R indices (all data) $R_1 = 0.0812$, $wR_2 = 0.1562$, gof 1.068, Largest difference peak and hole 0.268 and −0.312 e Å^{-3}.

Computational Details

Quantum mechanical calculations were performed in order to achieve deeper understanding regarding the nature and behavior of various non-covalent interactions. All the calculations were performed using the Gaussian03 package [19]. Initial geometries of the C–H···O and C–H···π bonded dimers and trimers were taken from the X-ray structure. Starting from these initial geometries all dimeric and trimeric motifs were optimized by keeping the interaction distances frozen. All calculations were performed at the density functional theory (DFT) level using B3LYP [20, 21] functional and 6-31G** basis set for all the atoms. The energies (ΔE_{dimer} and ΔE_{trimer}) for dimeric and trimeric motifs involving the 2 and 3 molecules, respectively were calculated using the formula $\Delta E_{\text{dimer}} = E_{\text{dimer}} - (2 \times E_{\text{monomer}})$ and $\Delta E_{\text{trimer}} = E_{\text{trimer}} - (3 \times E_{\text{monomer}})$, where E_{monomer}, E_{dimer}, E_{trimer}- are the energies of the monomer, dimer and trimer motifs, respectively. E_{monomer} was calculated by optimizing a single molecule at the same level of theory. The intermolecular interaction strengths are significantly weaker than either ionic or covalent bonding, therefore it was essential to do basis set superposition error (BSSE) corrections. The BSSE corrections in the interaction energies were done using Boys–Bernardi scheme. In this paper all the interaction energies have been reported after BSSE correction [22].

Hirshfeld Surface Analysis

Molecular Hirshfeld surfaces [23] in the crystal structure were constructed on the basis of the electron distribution calculated as the sum of spherical atom electron densities [24, 25]. For a given crystal structure and a set of spherical atomic densities, the Hirshfeld surface is unique [26]. The normalized contact distance (d_{norm}) based on both d_e and d_i (where d_e is distance from a point on the surface to the nearest nucleus outside the surface and d_i is distance from a point on the surface to the nearest nucleus inside the surface) and the vdW radii of the atom, as given by Eq. 1 enables identification of the regions of particular importance to intermolecular interactions [22]. The combination of d_e and d_i in the form of two-dimensional (2D) fingerprint plot [27, 28] provides a summary of intermolecular contacts in the crystal [22]. The Hirshfeld surfaces mapped with d_{norm} and 2D fingerprint plots were generated using the Crystal-Explorer 2.1 [29]. Graphical plots of the molecular Hirshfeld surfaces mapped with d_{norm} used a red-white-blue colour scheme, where red highlight shorter contacts, white represents the contact around vdW separation, and blue is for longer contact. Additionally, two further coloured plots representing shape index and curvedness based on local curvatures are also presented in this paper [30].

$$d_{\text{norm}} = \frac{d_i - r_i^{\text{vdW}}}{r_i^{\text{vdW}}} + \frac{d_e - r_e^{\text{vdW}}}{r_e^{\text{vdW}}} \quad (1)$$

Synthesis

The α-naphthol (1.44 g, 10 mmol) and dihydro-furan-2-one (0.86 g, 10 mmol) were dissolved in 50 mL ethanol and to it was added sodium ethoxide (0.80 g 11.7 mmol) in portions. The whole mixture was stirred with reflux for 4 h and finally the mixture was poured on the crushed ice and then neutralized with dil. HCl to obtain the solid product 2-(Naphthalen-1-yloxy)-butyric acid. The product was then dissolved in Eaton's reagent [31] and heated up to 50 °C for 2 h to obtain the crude final title compound. The solution was transferred to separating funnel and to this was added 200 mL of distilled water in dropwise manner and shaken with precaution to ensure hydrolysis of methanesulfonic anhydride. After complete hydrolysis of methanesulfonic anhydride the product was extracted with dichloromethane (2 × 100 mL). The extract was washed once with dilute aqueous sodium bicarbonate (100 mL) and twice with water, dried over sodium sulphate and concentrated. The concentrated solution was allowed to evaporate slowly to obtain the crystalline pure form of the title compound (yield 1.49 g, 70 %).

^{1}H NMR (300.40 MHz, $CDCl_3$) δ 8.37 (d, 1H, Ph), δ 7.80–7.83 (d, 1H, Ph), δ 7.50–7.62 (m, 4H, Ph), δ 4.45–4.49 (t, 2H, CH_2–CO), δ 2.99–3.04 (t, 2H, –CH_2–O), δ 2.30–2.39 (q, 2H, –CH_2–). $\nu_{\max}$(KBr)/cm^{-1} 1,700 (C=O). Anal. Calc. for $C_{14}H_{12}O_2$: C, 79.23; H, 5.70 %. Found: C, 79.85; H, 5.93 %. ESI–MS (m/z): 213.31 (M^+).

Scheme 1 Synthetic route for 9,10-Dihydro-8H-11-oxa-cyclohepta[*a*]naphthalen-7-one

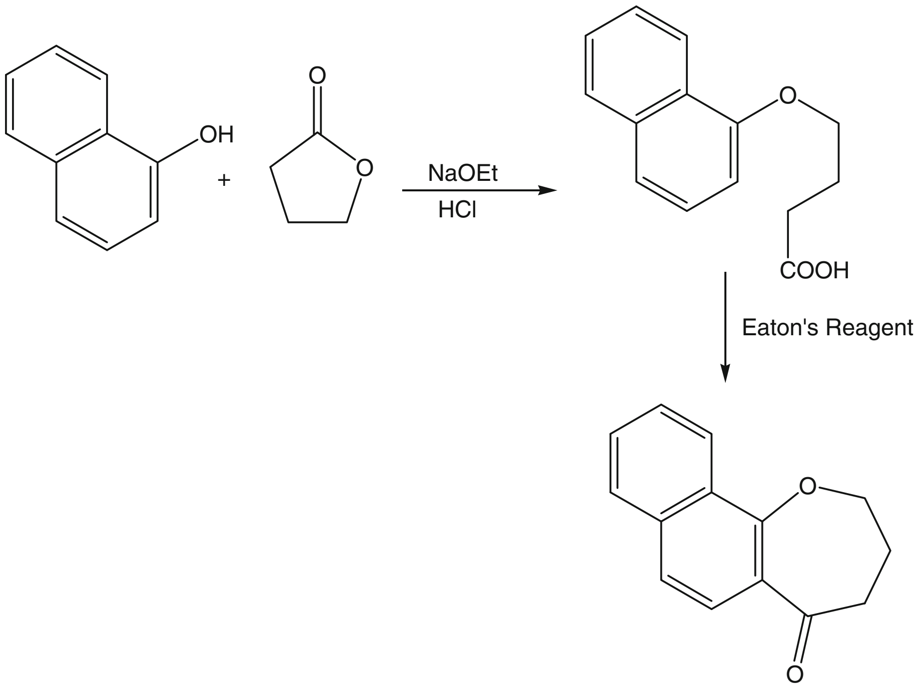

Results and Discussion

Synthesis

The reaction between α-naphthol and dihydro-furan-2-one in the presence of strong base yielded 4-(Naphthalen-1-yloxy)-4-butryic acid which on further treatment with Eaton's reagent [31] produced the final title compound (Scheme 1). The previous synthetic methodology using polyphosphoric acid [11] involved relatively higher temperature and time for cyclization in comparison to the synthesis reported herein. The obtained title compound was air as well moisture insensitive and was characterized spectroscopically and crystallographically.

Spectroscopy

The IR spectrum of the title compound displays some common features as far as naphthalen-7-one is concerned. The band arising at ~1,700 cm^{-1} is arising because of the *v* C=O group. The purity and composition of the title compound was checked by ^{1}H NMR spectroscopy in $CDCl_3$. The signals in the range δ 7.50–8.40 ppm are indicative of the presence of the aromatic protons. The triplets observed at δ 2.99–3.04 and δ 4.45–4.50 ppm can be assigned to the methylene protons of CH_2–CO and CH_2–O groups, while the multiplet arising at δ 2.30–2.39 is due to the methylene group flanked by CH_2–CO and CH_2–O groups.

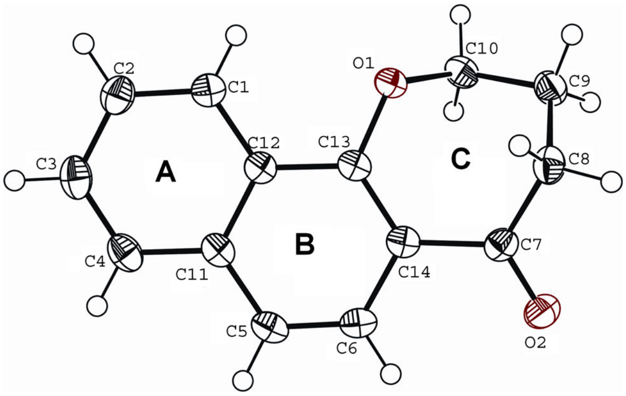

Fig. 1 ORTEP view with atom numbering scheme for title compound with displacement ellipsoids at the 50 % probability level

Molecular Structure Description

The crystals of the title compound suitable for single crystal X-ray diffraction were obtained by the slow evaporation method in dichloromethane solution. The title compound (Fig. 1) crystallized in the orthorhombic system with *P*bca space group and the pertinent hydrogen bond parameters are presented in Table 1. The fused naphthyl rings **A** and **B** are perfectly planar while the seven membered ring **C** posses puckered structure owing to the presence of heteroatom oxygen O1 as well as the three saturated carbon centers C8, C9 and C10. The atoms O1 and C9 are lying in the plane formed by the naphthyl ring,

Table 1 Hydrogen bond parameters for the title compound

D–H···A–X	*d* H···A (Å)	*d* D···A (Å)	*θ* D–H···A°
C(8)–H(8B)····O(2)^{a}	2.542	3.329	138.3
C(9)–H(9A)····O(2)^{b}	2.647	3.385	133.1
C(10)–H(10B)····O(1)^{c}	2.659	3.602	164.2
C(5)–H(5)····C(1)^{d}	2.857	3.751	161.4
H(5)–C(1)····C(4)^{d}			113.1

symmetry equivalents: ^{a} 2 − *x*, 0.5 + *y*, 0.5 − *z*; ^{b} 1.5 − *x*, 0.5 + *y*, *z*; ^{c} 1.5 − *x*, −0.5 + *y*, *z*; ^{d} 0.5 + *x*, 1.5 − *y*, 1 − *z*

while the carbonyl carbon C7 is deviated by 0.28 Å from the fused ring's plane. The saturated carbon center C8 is deviating by 0.77 Å whereas C10 is displaying deviation by −1.02 Å. The torsion angles C13–O1–C10–C9, C(10)–O(1)–C(13)–C(14) and C(10)–O(1)–C(13)–C(12) are −91.98(16)°, 42.7(2)° and −136.80(14)°, respectively.

The supramolecular aggregation of the title compound is stabilized by a combination of several weak interactions out of which C–H···π and C–H···O interactions are most important (Figs. 2 and 3, respectively). The weak C–H···π interaction leads to the form a single helical motif along *b* axis having C(5)–H(5)···C(1)(π) distance 2.857 Å (symm. op. 0.5 + *x*, 1.5 − *y*, 1 − *z*). The another important C–H···O interaction also generates linear chains along *a* axis and unlike C–H···π interaction, in this case there are pair of C–H···O interactions viz. C(8)–H(8B)···O(2), C(9)–H(9A)···O(2) and C(10)–H(10B)···O(1) interactions having distances 2.647, 2.659 and 2.857 Å, respectively (symm. op. 2−*x*, 0.5 + *y*, 0.5 − *z*; 1.5 − *x*, 0.5 + *y*, *z*; 1.5 − *x*, −0.5 + *y*, *z*). Of these interactions C(10)–H(10B)···O(1) is the most significant as it is close to linear. These interaction distances are in accordance with those reported previously for the analogous systems [32, 33].

DFT Results Regarding Non-covalent and π-Stacked Motifs

The crystal structure of the title compound as discussed above is a good example of the interplay of different molecular interactions that lead to interesting supramolecular aggregates in the solid state. In order to analyze the

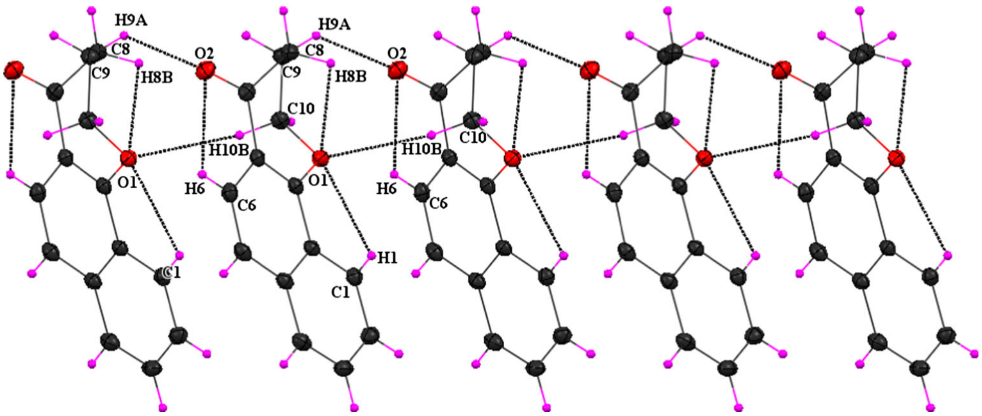

Fig. 2 Weak C–H···O interactions lead to linear chains along *a* axis

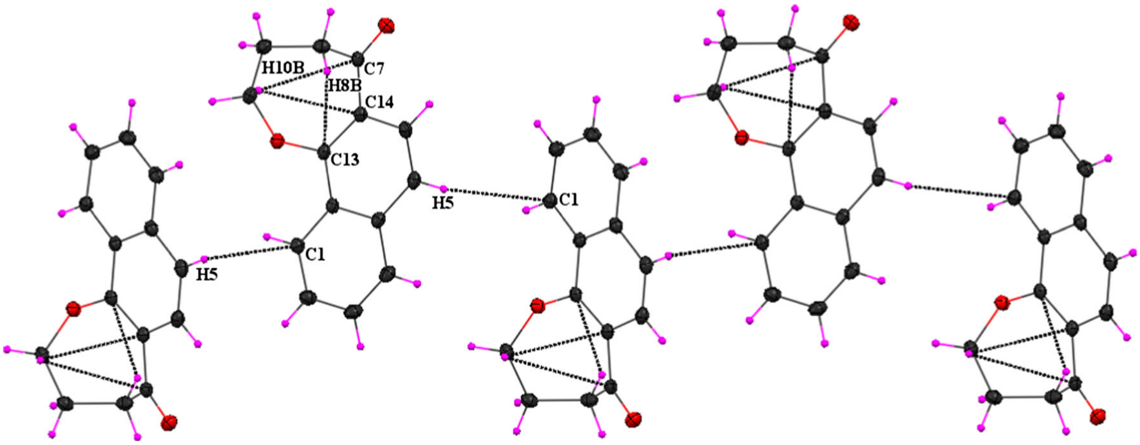

Fig. 3 Weak C–H···π interactions lead to single helical motif along *b* axis

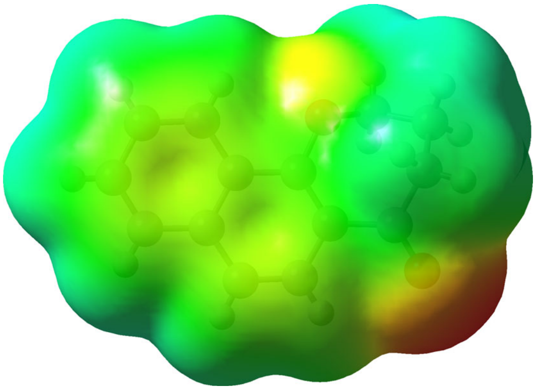

Fig. 4 Electrostatic potential surface for the title complex, *red* region indicates the electron rich while *blue-green* region is indicative of the electron deficient sites (Color figure online)

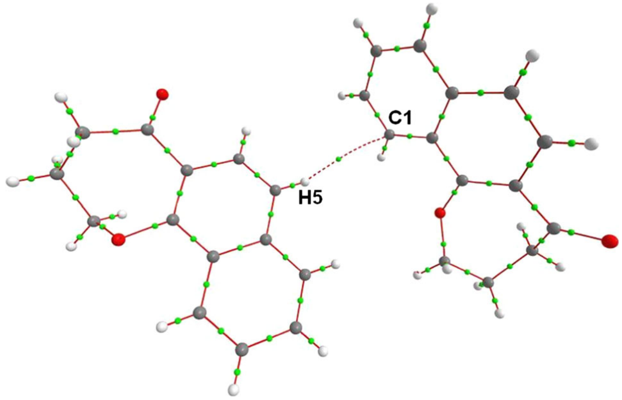

Fig. 5 Molecular graph of the dimer held by C–H···π interaction calculated by AIM using B3LYP/6-31G** level of theory

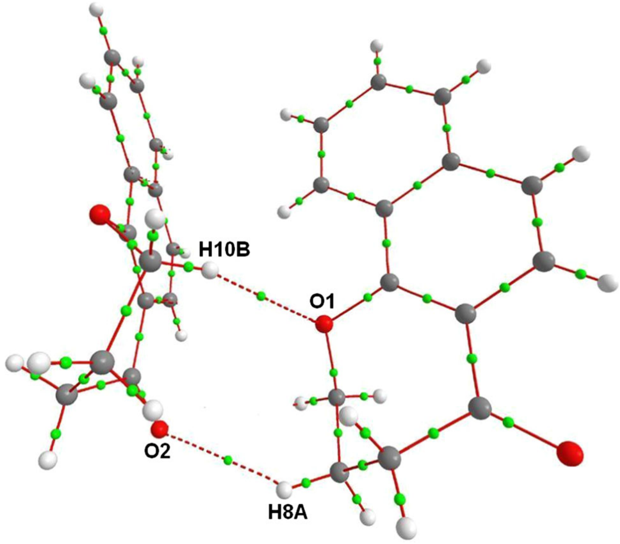

Fig. 6 Molecular graph of the dimer held by C–H···O interaction calculated by AIM using B3LYP/6-31G** level of theory

various interaction that lead to the crystal structure, interaction energies and electrostatic potentials have been calculated for dimer and trimer fragments keeping C–H···O, C–H···π distances fixed as obtained from X-ray single-crystal structure analysis (Fig. 4). The analysis of the interaction energy in the crystal structure of the title compound by means of dimer unit at the DFT level of theory yields the interaction energy in the C–H···O dimer of −14.19 kJ/mol and those calculated for C–H···π interaction gives −13.91 kJ/mol. The interaction energy for the trimer motif inculcating both C–H···O and C–H···π interactions gives the value −27.24 kJ/mol. The interaction energy calculations for both the dimer and trimer units indicate that both C–H···O and C–H···π interactions display no cooperative effects.

To confirm further the existence of C–H···O and C–H···π interactions, bond critical points (bcp) were calculated for the dimer (Figs. 5, 6) as well as the trimer (Fig. 7) by using the Atoms in Molecules theory [34]. The bond critical points observed between the H and O as well as between H and C atoms confirm the presence of C–H···O and C–H···π interactions between two molecules of the title compound (Figs. 5, 6 and 7). The value of electron density (ρ); Laplacian ($\nabla^2\rho_{bcp}$); bond ellipticity (ε) and total energy density (H) at the bond critical point for C–H···O and C–H···π interactions for the compound is presented in Table 2. From the Table 2 it is evident that the electron density for all the types of interactions at bond critical point (ρ_{bcp}) are less than +0.10 au which indicates a closed shell hydrogen bonding interactions. Additionally, the Laplacian of the electron density $\nabla^2\rho_{bcp}$ in all the three cases are greater than zero which indicates the depletion of electron density in the region of contact between the H···O and H···C atoms. The bond ellipticity (ε) measures the extent to which the density is preferentially accumulated in a given plane containing the bond path. The ε values for all the three compounds indicate that these C–H···O and C–H···π interactions are not cylindrically symmetrical in nature.

Hirshfeld Surface Analysis

The Hirshfeld surfaces of title compound are illustrated in Fig. 8, showing surfaces that have been mapped over a d_{norm} range of −0.5 to 1.5 Å, shape index (−1.0 to 1.0 Å) and curvedness (−4.0 to 0.4 Å). The surfaces are shown as transparent to allow visualization of the aromatic as well as the puckered ring moieties around which they were calculated. The weak interaction information discussed in

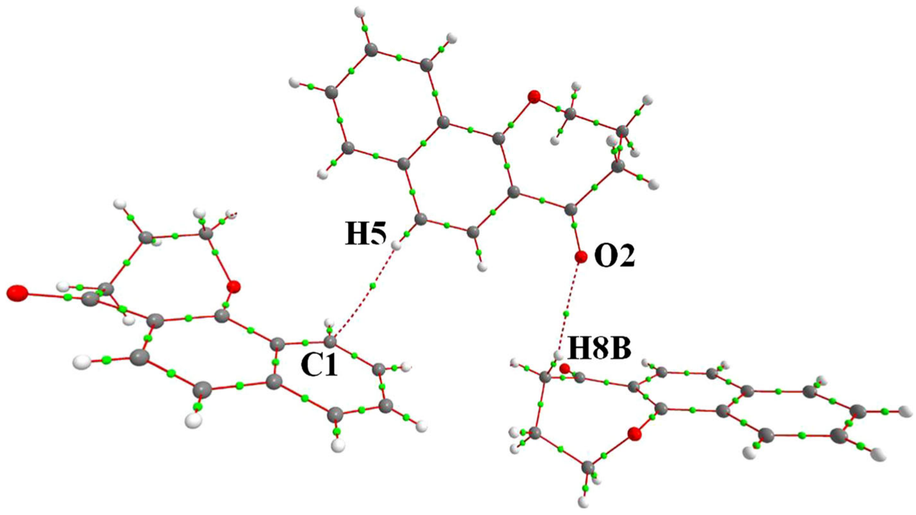

Fig. 7 Molecular graph of the trimer held by C–H···O and C–H···π interaction calculated by AIM using B3LYP/6-31G** level of theory

Table 2 Selected topographical features of C–H···O and C–H···π interactions computed at B3LYP/6-31G** level of theory for dimer and trimer

Number of molecular units	Interaction type	ρ_{bcp}	$\nabla^2\rho_{bcp}$	ε	H (au)
Dimer	C–H5···C1(π)	+0.005268	+0.015808	+0.461309	+0.045661
Dimer	C–H10B···O1	+0.005657	+0.023091	+0.401216	+0.095784
	C–H8B···O2	+0.006579	+0.024618	+0.157800	+0.025925
Trimer	C–H8B···O2	+0.007400	+0.028941	+0.420520	+0.023430
	C–H5···C1(π)	+0.005261	+0.015805	+0.464152	+0.046033

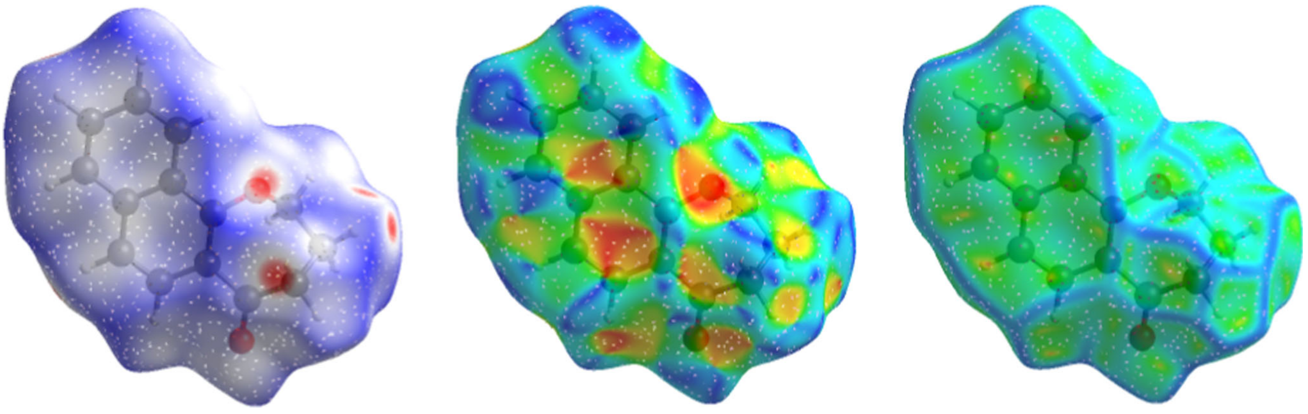

Fig. 8 Hirshfeld surfaces mapped with d_{norm} (*left*), shape index (*middle*) and curvedness (*right*) for the title compound

X-ray crystallography section is summarized effectively in the spots, with the large circular depressions (deep red) visible on the d_{norm} surfaces indicative of hydrogen bonding contacts. The dominant interactions between C–H···O and C–H···π interactions for the compound can be seen in Hirshfeld surface plots as the bright red shaded area in Fig. 8. The small extent of area and light color on the surface indicates weaker and longer contact other than hydrogen bonds.

The fingerprint plots for title compound are presented in Fig. 9. The C–H···O and C–H···π intermolecular interactions appear as two distinct spikes of almost equal lengths in the 2D fingerprint plots in the region 2.03 Å < (d_e + d_i) < 2.47 Å as light sky-blue pattern in full fingerprint 2D plots. Complementary regions are visible in the fingerprint plots where one molecule acts as a donor ($d_e > d_i$) and the other as an acceptor ($d_e < d_i$). The fingerprint plots can be decomposed to highlight particular atom pair close contacts. This decomposition enables separation of contributions from different interaction types, which overlap in the full fingerprint. The proportions of C–H···O/C–H···O interactions comprising 17.5 % of the

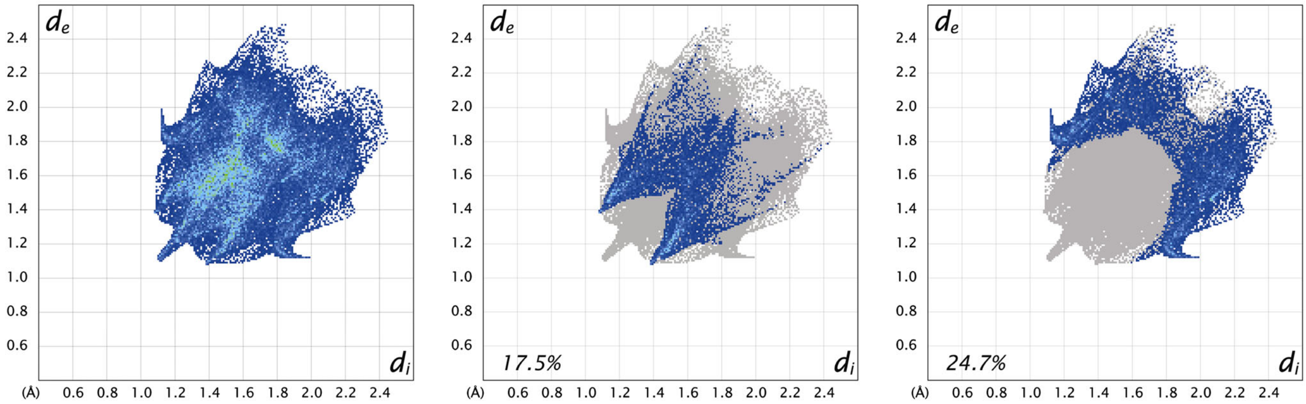

Fig. 9 Fingerprint plots Full (*left*), resolved into C–H···O/C–H···O (*middle*) and C–H···π/π···H–C (*right*) the title compound showing percentages of contact contributed to the total Hirshfeld surface area of the molecules

total Hirshfeld surface, while the proportion of C–H···π/π···H–C interactions comprises of 24.7 % of the total Hirshfeld surface for each molecule of the title compound.

Conclusion

Here we have synthesized and characterized the compound using elemental analysis, IR, ^{1}H NMR, mass spectrometry and finally by X-ray crystallography. As crystal data suggested for interactions such as Ar–H···π and C–H···π are non-covalent, we have also done computational studies to get deeper insights. The results from DFT calculations have shown that indeed the interactions does play greater role specially in making very large supramolecules and also have quantitative estimate of −27.24 kJ/mol for these interactions. Apart from DFT we also have carried out AIM calculations and Hirshfeld surfaces analysis for the confirmation of the C–H···O and C–H···π interactions. Hirshfeld calculations estimate C–H···O/C–H···O interactions (17.5 %) and C–H···π/π···H–C interactions (24.7 %) of total Hirshfeld surface for each molecule. We conclude that these studies provide us with great deal of information regarding weak interactions and in designing of supramolecules with non-bonded interactions in these types of organic systems.

Supplementary Information

CCDC 892399 contains the supplementary crystallographic data for the title compound. These data can be obtained free of charge via http://www.ccdc.cam.ac.uk/conts/retrieving.html, or from Cambridge Crystallographic Data Center, 12 Union Road, Cambridge CB2 1EZ, UK; fax (+44) 1223-336-033; or email: deposit@ccdc.cam.ac.uk. CCDC contain the supplementary crystallographic data for the complex.

Acknowledgments A.K is grateful to Department of Science and Technology, New Delhi for the financial assistance in the form of project No. SB/FT/CS-018/2012.

Conflict of interest Authors declare that they have no conflict of interest.

References

1. Lehn JM (1995) Supramolecular chemistry. VCH, Weinheim
2. Lehn JM (1990) Chem Int Ed 29:1304–1319
3. Badjić JD, Nelson A, Cantrill SJ, Turnbull WB, Stoddart JF (2005) Acc Chem Res 38:723–732
4. Descalzo AB, Martinez-Manez R, Sancenon R, Hoffmann K, Rurak K (2006) Angew Chem Int Ed 45:5924–5948
5. Gamez P, Mooibroek TJ, Teat SJ, Reedjik J (2007) Acc Chem Res 40:435–444
6. Katz MJ, Sakai K, Leznoff DB (2008) Chem Soc Rev 37:1884–1895
7. Metrangolo P, Meyer F, Pilati T, Resnati G, Terraneo G (2008) Angew Chem Int Ed 47:6114–6127
8. Schneider HJ (2009) Angew Chem Int Ed 48:3924–3977
9. Schmidbaur H, Schier A (2008) Chem Soc Rev 37:1931–1951
10. Kuntz ID, Blaney JM, Oatley SJ, Langridge R, Ferrin TE (1982) J Mol Biol 161:269–288
11. Tandon VK, Chhor RB, Goswami GK (1998) Indian J Chem Sect B 37B:1027–1029
12. Balasubramanium M, Rammana DV, Ramdas SR (1986) Sulfur Lett 4:197–201
13. Cagniant P, Charaux C (1996) Bull de la Soc Chim de Fr 10:3249–3258
14. Fontaine G (1968) Ann de Chim 14:179–191
15. Mandal AN, Bhattacharya S (1984) Indian J Chem Sect B 23B:736–742
16. *SAINT* + 6.02 ed. (1999) Bruker AXS; Madison
17. Farrugia LJJ (1999) Appl Cryst 32:837–838
18. Burnett MN, Johnson CK (1996) ORTEP-III: Oak Ridge thermal ellipsoid plot program for crystal structure illustrations, Report ORNL-6895, Oak Ridge National Laboratory, Oak Ridge

19. Frisch MJ, Trucks GW, Schlegel HB, Scuseria GE, Robb MA, Cheeseman JR, Montgomery JA, Vreven Jr T, Kudin KN, Burant JC, Millam JM, Iyengar SS, Tomasi J, Barone V, Mennucci B, Cossi M, Scalmani G, Rega N, Petersson GA, Nakatsuji H, Hada M, Ehara M, Toyota K, Fukuda R, Hasegawa J, Ishida M, Nakajima T, Honda Y, Kitao O, Nakai H, Klene M, Li X, Knox JE, Hratchian HP, Cross JB, Bakken V, Adamo C, Jaramillo J, Gomperts R, Stratmann RE, Yazyev O, Austin AJ, Cammi R, Pomelli C, Ochterski JW, Ayala PY, Morokuma K, Voth GA, Salvador P, Dannenberg JJ, Zakrzewski VG, Dapprich SD, Daniels A, Strain MC, Farkas O, Malick DK, Rabuck AD, Raghavachari K, Foresman JB, Ortiz JV, Cui Q, Baboul AG, Clifford S, Cioslowski J, Stefanov BB, Liu G, Liashenko A, Piskorz P, Komaromi I, Martin RL, Fox DJ, Keith T, Al-Laham MA, Peng CY, Nanayakkara A, Challacombe M, Gill PMW, Johnson B, Chen W, Wong WM, Gonzalez C, Pople JA (2004) Gaussian 03 (Revision D. 01), Gaussian, Inc., Wallingford
20. Becke AD (1993) J Chem Phys 98:5648–5652
21. Lee CT, Yang WT, Parr RG (1998) Phys Rev B: Condens Matter Mater Phys 37:785–788
22. Boys SF, Bernardi F (1970) Mol Phys 19:553–566
23. Spackman MA, McKinnon JJ (2002) CrystEngComm 4:378–392
24. Spackman MA, Byrom PG (1997) Chem Phys Lett 267:309
25. McKinnon JJ, Mitchell AS, Spackman MA (1998) Chem-Eur J 4:2136–2141
26. McKinnon JJ, Spackman MA, Mitchell AS (2004) Acta Crystallogr Sect B 60:627–668
27. Rohl AL, Moret M, Kaminsky W, Claborn K, McKinnon JJ, Kahr B (2008) Cryst Growth Des 8:4517–4525
28. Parkin A, Barr G, Dong W, Gilmore CJ, Jayatilaka D, McKinnon JJ, Spackman MA, Wilson CC (2007) CrystEngComm 9:648–652
29. Wolff SK, Greenwood DJ, McKinnon JJ, Jayatilaka D, Spackman MA (2007) Crystal Explorer 2.0. University of Western Australia, Perth
30. Koenderink JJ, van Doorn AJ (1992) Image Vis Comput 10:557–564
31. Eaton PE, Carlson GR, Lee JT (1973) J Org Chem 38:4071–4073
32. Desiraju G, Steiner T (1999) The weak hydrogen bond in structural chemistry and biology. Oxford University Press, Oxford
33. García-Báez EV, Martínez-Martínez FJ, Höpfl H, Martínez IIP (2003) Cryst Growth Des 3:35–45
34. Bader RFW (1990) Atoms in molecules: a quantum theory. Oxford University Press, New York